International Immunopharmacology 74 (2019) 105701

Contents lists available at ScienceDirect

International Immunopharmacology

journal homepage: www.elsevier.com/locate/intimp

Dihydroartemisinin derivative DC32 inhibits inflammatory response in osteoarthritic synovium through regulating Nrf2/NF-κB pathway

Ya-Nan Li[a,1], Meng-Lin Fan[a,1], Han-Qing Liu[a], Bin Ma[a], Wen-Ling Dai[a], Bo-Yang Yu[a,b,*], Ji-Hua Liu[a,**]

[a] Jiangsu Key Laboratory of TCM Evaluation and Translational Research, School of Traditional Chinese Pharmacy, China Pharmaceutical University, Nanjing, Jiangsu, China
[b] State Key Laboratory of Natural Medicines, China Pharmaceutical University, Nanjing, Jiangsu, China

ARTICLE INFO

Keywords:
DC32
Osteoarthritis (OA)
Synovitis
Fibroblast-like synoviocytes (FLSs)
Nrf2/NF-κB pathway

ABSTRACT

Synovitis is an aseptic inflammation that leads to joint effusion, pain and swelling. As one of the main drivers of pathogenesis in osteoarthritis (OA), the presence of synovitis contributes to pain, incidence and progression of OA. In our previous study, DC32 [(9α,12α-dihydroartemisinyl) bis(2′-chlorocinnmate)], a dihydroartemisinin derivative, was found to have an antirheumatic ability via immunosuppression, but the effect of DC32 on synovitis has not been fully illuminated. In this study, we chose to evaluate the effect and mechanism of DC32 on attenuating synovial inflammation. Fibroblast-like synoviocytes (FLSs) of papain-induced OA rats were isolated and cultured. And DC32 significantly inhibited the invasion and migration of cultured OA-FLSs, as well as the transcription of IL-6, IL-1β, CXCL12 and CX3CL1 in cultured OA-FLSs measured by qPCR. DC32 remarkably inhibited the activation of ERK and NF-κB pathway, increased the expression of Nrf2 and HO-1 in cultured OA-FLSs detected by western blot. DC32 inhibited the degradation and phosphorylation of IκBα which further prevented the phosphorylation of NF-κB p65 and the effect of DC32 could be relieved by siRNA for Nrf2. In papain-induced OA mice, DC32 significantly alleviated papain-induced mechanical allodynia, knee joint swelling and infiltration of inflammatory cell in synovium. DC32 upregulated the mRNA expression of Type II collagen and aggrecan, and downregulated the mRNA expression of MMP2, MMP3, MMP13 and ADAMTS-5 in the knee joints of papain-induced OA mice measured by qPCR. The level of TNF-α in the serum and secretion of TNF-α in the knee joints were also reduced by DC32 in papain-induced OA mice. In conclusion, DC32 inhibited the inflammatory response in osteoarthritic synovium through regulating Nrf2/NF-κB pathway and attenuated OA. In this way, DC32 may be a potential agent in the treatment of OA.

1. Introduction

Osteoarthritis (OA), a universal disabling joint disease, is characterized by degeneration of the articular cartilage, subchondral osteoporosis and synovitis [1]. OA is increasingly recognized as a disorder of the entire joint, in which inflammation plays a prominent role, manifesting as synovitis [2,3]. The presence of synovitis has been associated with pain, incidence and progression of OA [4]. Therefore, nonsteroidal anti-inflammatory drugs (NSAIDs) and analgesic drugs are commonly used in attenuating OA.

Many inflammatory mediators such as proteinases, growth factors and cytokines are involved in the initial stages of OA [5]. As one of the drivers of OA pathogenies, synovial inflammation leads to an imbalance between the catabolic and anabolic activities of the chondrocyte in the cartilage extracellular matrix (ECM), causing the dysregulation of chondrocyte function [6,7]. The synovium in OA patients is characterized by synovial lining hyperplasia, sublining fibrosis and stromal vascularization [8]. The infiltration of inflammatory cells in synovium

Abbreviations: OA, osteoarthritis; FLSs, fibroblast-like synoviocytes; NSAIDs, nonsteroidal anti-inflammatory drugs; ECM, extracellular matrix; IL, interleukin; MMP, matrix metalloproteinase; Nrf2, NF-E2-related factor 2; CIA, collagen-induced arthritis; 9-OH DHA, 9α-hydroxyl-dihydroartemisinin; qPCR, quantitative polymerase chain reaction; Col2a1, type II collagen; MAPK, mitogen-activated phosphokinase

* Correspondence to: B.-Y. Yu, Jiangsu Key Laboratory of TCM Evaluation and Translational Research, School of Traditional Chinese Pharmacy, China Pharmaceutical University, Nanjing, Jiangsu, China.
** Corresponding author.
E-mail addresses: boyangyucpu@163.com (B.-Y. Yu), liujihua@cpu.edu.cn (J.-H. Liu).
[1] These authors contributed equally to this work.

https://doi.org/10.1016/j.intimp.2019.105701
Received 21 April 2019; Received in revised form 5 June 2019; Accepted 13 June 2019
Available online 19 June 2019

Table 1
Primer sequences used in qPCR experiments.

Gene	Species	Forward primer (5′–3′)	Reverse primer (5′–3′)
IL-6	Rat	AATCTGCTCTGGTCTTCTGG	GATGAGTTGGATGGTCTTGG
IL-1β	Rat	CCAGGATGAGGACCCAAGCA	TCCCGACCATTGCTGTTTCC
CXCL12	Rat	TGCTCATCTCTGTCTCATCC	CATTGGTCATGGAGGTCAAC
CX3CL1	Rat	TGGTCTACTCTTCTGTCTGG	CTGTCTGAATCACACTCTGG
GAPDH	Rat	CAGGGCTGCCTTCTCTTGTG	GATGGTGATGGGTTTCCCGT
MMP2	Mouse	ATTTGGCGGACAGTGACACCAC	ATCTACTTGCTGGACATCAGGGGG
MMP3	Mouse	GCTGAGGACTTTCCAGGTGTTG	GGTCACTTTTTTGGCATTTGGGTC
MMP13	Mouse	GATGACCTGTCTGAGGAAG	ATCAGACCAGACCTTGAAG
ADAMTS-5	Mouse	TCTCCAAAGGTTACGGATGGG	TCTTCAGGGCTAAGTAGGCAG
Aggrecan	Mouse	CACGCTACACCCTGGACTTTG	CCATCTCCTCAGCGAAGCAGT
Col2a1	Mouse	AGCGACTGTCCCTCGGAAAAAC	CCAGGTAGGCGATGCTGTTCTTAC
TNF-α	Mouse	GTTCTATGGCCCAGACCCTCAC	GGCACCACTAGTTGGTTGTCTTTG
GAPDH	Mouse	TGATGGGTGTGAACCACGAG	GCCCTTCCACAATGCCAAAG

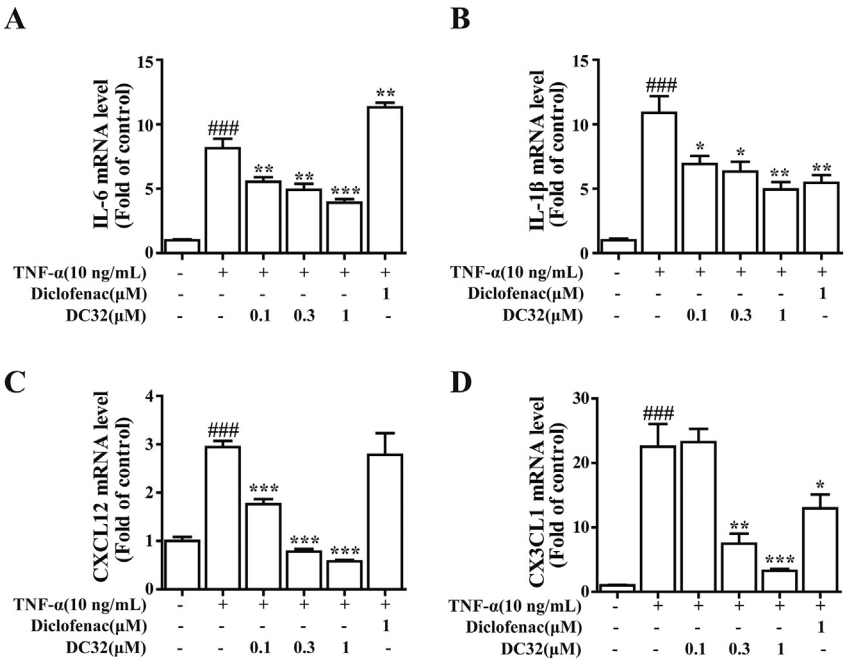

Fig. 1. DC32 decreased the mRNA levels of pro-inflammatory cytokines and chemokines in cultured OA-FLSs. OA-FLSs of papain-induced OA rats were isolated and cultured. OA-FLSs were treated with TNF-α (10 ng/mL) and various concentrations of DC32 (0.1, 0.3 and 1 μM) for 24 h. The relative levels of IL-6 (A), IL-1β (B), CXCL12 (C), and CX3CL1 (D) mRNA expression in cultured OA-FLSs were measured by qPCR. The data generated are from 3 replicate experiments. n = 5, values are the mean ± SEM. $^{###}P < 0.001$ vs. the Control group, $^{*}P < 0.05$, $^{**}P < 0.01$, $^{***}P < 0.001$ vs. the TNF-α group.

observed in OA patients can amplify synovial inflammation [9,10]. Chemokines such as CXCL12 and CX3CL1 promote the chemotactic recruitment of leukocytes to the site of inflammation and accelerate the inflammatory response [11].

TNF-α, commonly detected in synovial fluid in OA patients, could be used to stimulate fibroblast-like synoviocytes (FLSs) and activate a series of downstream signaling pathways, including mitogen-activated phosphokinase (MAPK) and NF-κB [12–15]. FLSs in the inflamed synovium produce catabolic and pro-inflammatory mediators, leading to excess production of the proteolytic enzymes, which exacerbate cartilage breakdown and OA deterioration [16–18]. The NF-κB signaling pathway is one of the crucial pathways that regulates the transcription of the pro-inflammatory cytokines [19]. Activation of NF-κB signaling also accelerates the secretion of matrix metalloproteinases (MMPs), ADAMTSs and chemokines and ultimately enhances articular damage [20,21]. However, NF-κB signaling induced inflammation could be attenuated by activating NF-E2-related factor 2 (Nrf2) - antioxidant signaling, which regulates the expression of crucial antioxidant and anti-inflammatory genes [22].

Artemisinin and its derivatives are widely used antimalaria drugs with antiviral and anti-inflammatory activities [23,24]. In our previous studies, DC32 (Fig. 5A) was reported to restore the imbalance of the T lymphocyte subpopulation and ameliorate inflammatory symptoms by activating the Nrf2/HO-1 pathway in mice with collagen-induced arthritis (CIA) [25,26]. Focusing on the synovial inflammation, this study investigated the effects of DC32 on inflammatory responses in rat osteoarthritic synovium and the mechanism of DC32 on inhibiting synovitis.

2. Methods

2.1. Animals

Pathogen-free male Sprague-Dawley rats (n = 20, 6 weeks old, 200–220 g in weight) were purchased from the Center of Experimental Animals of Nantong University (Jiangsu, China). The rats were fed a standard laboratory diet with ultra-pure water and were housed under SPF conditions with a 12 h light/dark cycle.

Pathogen-free male C57BL/6J mice (n = 60, 6 weeks old, 20–22 g in weight) were purchased from Weitong Lihua Experimental Animal Co. Ltd. (Beijing, China). The mice were fed a standard laboratory diet with ultra-pure water and were housed under SPF conditions with a 12 h light/dark cycle.

2.2. Preparation of DC32

DC32 was prepared as previously described [27]. In brief, dihydroartemisinin (DHA) was biotransformed to 9α-OH DHA by

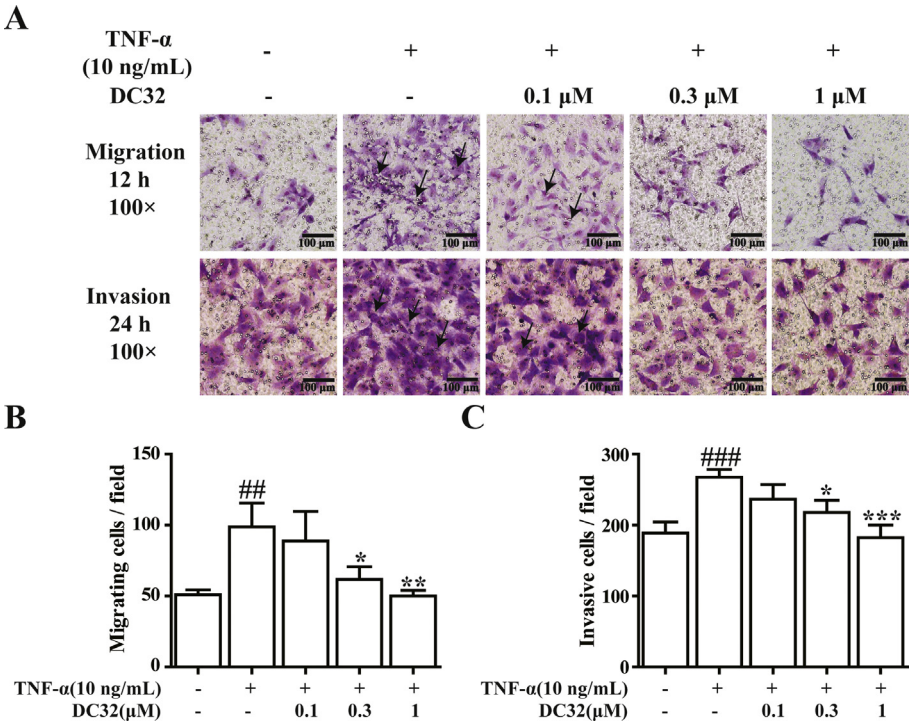

Fig. 2. DC32 inhibited TNF-α-induced migration and invasion of cultured OA-FLSs. OA-FLSs of papain-induced OA rats were isolated and cultured. Migration and invasion of cultured OA-FLSs was assessed in Transwell chambers. OA-FLSs were treated with TNF-α (10 ng/mL) and various concentrations of DC32 (0.1, 0.3 and 1 μM) for 12 h and 24 h. The representative graphs of migration and invasion of cultured OA-FLSs for 12 h and 24 h were shown in (A). The number of migrating OA-FLSs (B) and invasive OA-FLSs (C) were quantified respectively. The data generated are from 3 replicate experiments. n = 3, values are the mean ± SEM, $^{\#\#}P < 0.01$, $^{\#\#\#}P < 0.001$ vs. the Control group, $^{*}P < 0.05$, $^{**}P < 0.01$, $^{***}P < 0.001$ vs. the TNF-α group.

Streptomyces griseus ATCC 13273. Then, DC32 was synthesized by coupling 9α-OH DHA and 2-Cl cinnamic acid. After separation and purification, the purity of DC32 was determined by HPLC. DC32 with a purity > 99% was used in this research.

2.3. Induction of OA in SD rats

Preparation of L-cysteine-activated papain: papain was dissolved in sterile physiological saline to a concentration of 4%, and L-cysteine was dissolved in sterile physiological saline to a final concentration of 0.03 M [28,29]. Papain (4%) was mixed with 0.03 M L-cysteine at a ratio of 2: 1. Then the mixture was placed at room temperature for 30 min.

Male SD rats received a 0.2 mL intra-articular injection of L-cysteine-activated papain in knee joints on the 1st, 4th and 7th days to induce OA. After four weeks, papain-induced OA rats were sacrificed for OA-FLSs isolation. And OA-FLSs used in present research were all from SD rats.

2.4. Isolation and culture of primary rat OA-FLSs

In brief, synovial tissues from papain-induced OA rats were washed twice with phosphate-buffered saline and cut into small pieces. Then synovial tissues were digested for 40 min with 1 mg/mL collagenase (Sigma-Aldrich, USA) at 37 °C and then washed twice with DMEM-12% FBS (Sigma-Aldrich, USA). The adherent cells were allowed to attach to tissue culture plates overnight, and non-adherent cells were washed away with fresh medium once per day for the next 3 days, followed by repeated washing and the addition of fresh medium every 3 days for 2 weeks. Passages 3–6 were used for the experiments [30,31].

2.5. Cell viability

The cytotoxicity of DC32 on OA-FLSs was analyzed by MTT. In brief, OA-FLSs (7×10^3 cells/well) were seeded in 96-well plates and incubated for 12 h. DC32 (0.1, 0.3, 1, 3, 10 μM) was added and incubated for 24 h. Then the supernatant was discarded and 100 μL of 0.5 mg/mL MTT was added. After incubation for 3 h, the OD value was measured at a test wavelength of 570 nm and a reference wavelength of 650 nm.

2.6. Cell migration and invasion assays

2.6.1. Cell migration assay

For the cell migration assay, cell migration induced by TNF-α was determined using 6.5 mm Transwell chambers with 8 μm pores (Corning, USA). DMEM-10% FBS was placed in the lower chambers. OA-FLSs (3×10^3 cells/well) were seeded in the upper chambers in duplicate filters with TNF-α (10 ng/mL), and DC32 (0.1, 0.3, 1 μM) was added to the corresponding chambers for 12 h. The chambers were fixed and stained by diff-quick stain as described in the instructions.

2.6.2. Cell invasion assay

For the cell invasion assay, Matrigel basement membrane matrix (BD Biosciences, USA) was diluted 8-fold in DMEM and coated in the Transwell chambers. DMEM-10% FBS was placed in the lower chambers. OA-FLSs (1×10^4 cells/well) were seeded into the upper chambers in duplicate filters with TNF-α (10 ng/mL), and DC32 (0.1, 0.3, 1 μM) was added to the corresponding chambers for 24 h. The cells that invaded the basement membrane were fixed and stained by diff-quick stain.

Migration and invasion were quantified by counting the stained cells that migrated or invaded to the lower side of the filter using an optical microscope (Olympus IX53) (magnification 100×). Each chamber was photographed for nine random fields, and the stained cells were counted.

2.7. Stimulation of OA-FLSs with TNF-α

OA-FLSs (5×10^5 cells/well) were seeded into 6-well plates for 12 h, and then stimulated with 10 ng/mL TNF-α. DC32 (0.1, 0.3, 1 μM) and diclofenac sodium (1 μM) were added to the corresponding wells. The cells were cultured for 24 h before mRNA and protein extraction.

2.8. Gene knockdown in OA-FLSs

Predesigned small interfering RNA (siRNA) for Nrf2 (sense: GCAG

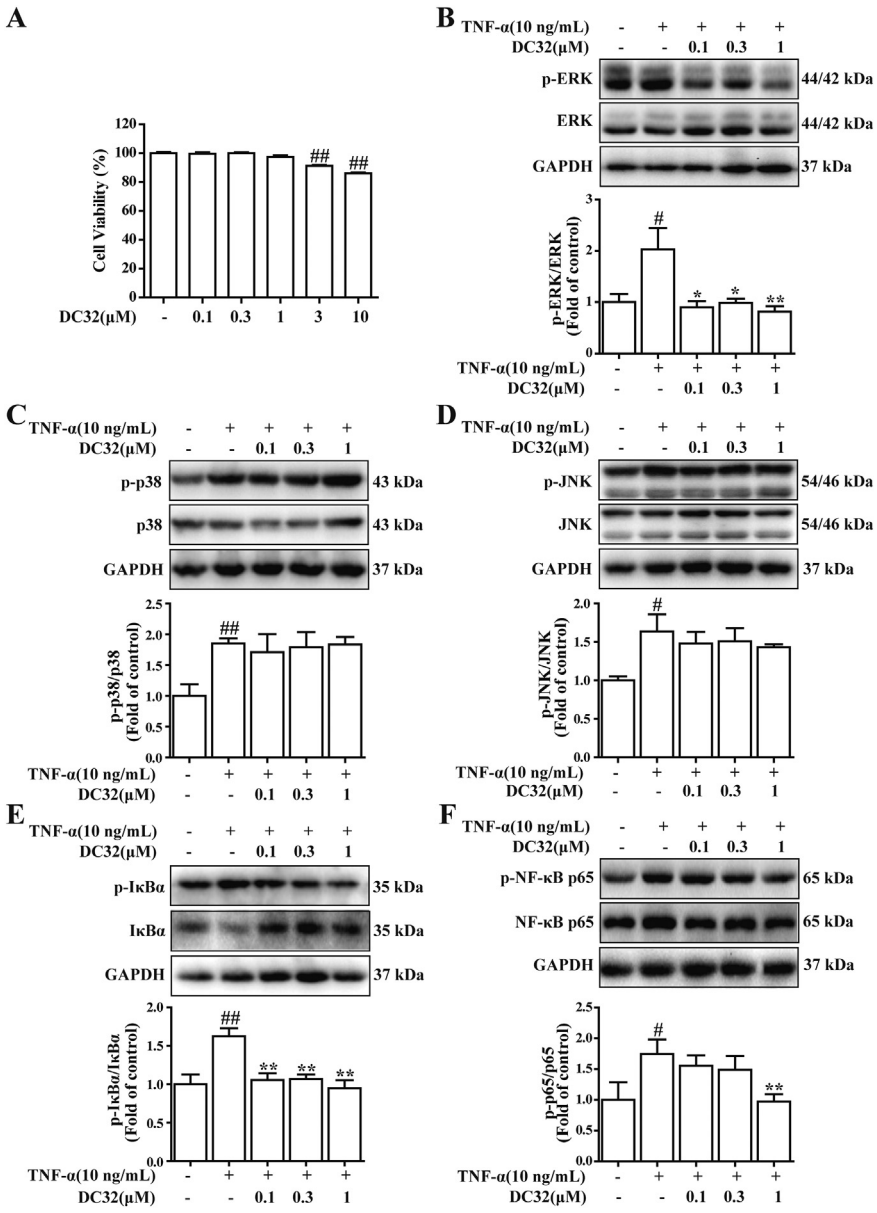

Fig. 3. DC32 inhibited the activation of ERK and NF-κB pathway in cultured OA-FLSs. OA-FLSs of papain-induced OA rats were isolated and cultured. OA-FLSs were cultured with increasing concentrations of DC32 (0.1, 0.3, 1, 3 and 10 μM) for 24 h. The cell viability of OA-FLSs was determined by MTT assay (A). OA-FLSs were treated with TNF-α (10 ng/mL) and various concentrations of DC32 (0.1, 0.3 and 1 μM) for 24 h. The phosphorylation of ERK (B), p38 (C) and JNK (D) were analyzed by western blot. Phosphorylation of ERK in cultured OA-FLSs was inhibited by DC32, but the phosphorylation of p38 and JNK were not affected by DC32. The phosphorylation of IκBα (E) and NF-κB p65 (F) were analyzed by western blot. DC32 (1 μM) significantly inhibited the phosphorylation and degradation of IκBα and the activation of NF-κB p65 in cultured OA-FLSs. The data generated are from 3 replicate experiments. n = 5, values are the mean ± SEM. $^{\#}P < 0.05$, $^{\#\#}P < 0.01$ vs. the Control group, $^{*}P < 0.05$, $^{**}P < 0.01$ vs. the TNF-α group.

CCAUGACUGAUUUAATT, antisense: UUAAAUCAGUCAUGGCUGCTT) and negative-control siRNA were purchased from TranSheepBio in China. Transfection mixes were prepared using Namipo. Cells at 30% confluence were transfected for 24 h and then treatment with DC32 (1 μM) or TNF-α (10 ng/mL). After cultured for another 24 h, the cells were collected for protein extraction.

2.9. Induction of OA in C57BL/6J mice

Male C57BL/6J mice were anesthetized with sodium pentobarbital (50 mg/kg, i.p.), and then received a 6 μL intra-articular injection of L-cysteine-activated papain in knee joints on the 1st, 4th and 7th days [32]. The mice were randomly divided into six groups of 10 mice to establish a Sham group, an OA group, DC32-treated groups ($6.25\ mg{\cdot}kg^{-1}{\cdot}d^{-1}$, $12.5\ mg{\cdot}kg^{-1}{\cdot}d^{-1}$, $25\ mg{\cdot}kg^{-1}{\cdot}d^{-1}$) and diclofenac sodium-treated group ($1\ mg{\cdot}kg^{-1}{\cdot}d^{-1}$). On day 14, DC32 and diclofenac sodium were administered p.o. to the OA mice every day for four weeks, while mice in the Sham and OA groups received vehicle. The above groups were used to evaluate the therapeutic effect of DC32 on OA.

The body weight of the mice was observed and measured every week. The diameter of the right knee joint was measured using electronic digital calipers every week. On day 42, the mice were sacrificed, and the knee joint was harvested for hematoxylin and eosin staining and protein extraction.

2.10. Mechanical allodynia (von Frey filaments)

Mechanical allodynia was assessed by measuring withdrawal thresholds to calibrated von Frey filaments. Mice were placed into a Perspex chamber with a metal grid floor, allowing access to the underside of their paws, and were allowed to acclimate prior to the start of the experiment. Mechanical allodynia was tested by touching the plantar surface of the mouse's hind paw with von Frey filaments in ascending order of force for up to 5 s. A positive response was noted if the paw was sharply withdrawn. Once a positive withdrawal response was established, the paw was retested starting with the next descending von Frey filament until no response occurred. The lowest amount of force required to elicit a response was recorded as the paw withdrawal threshold in grams [33].

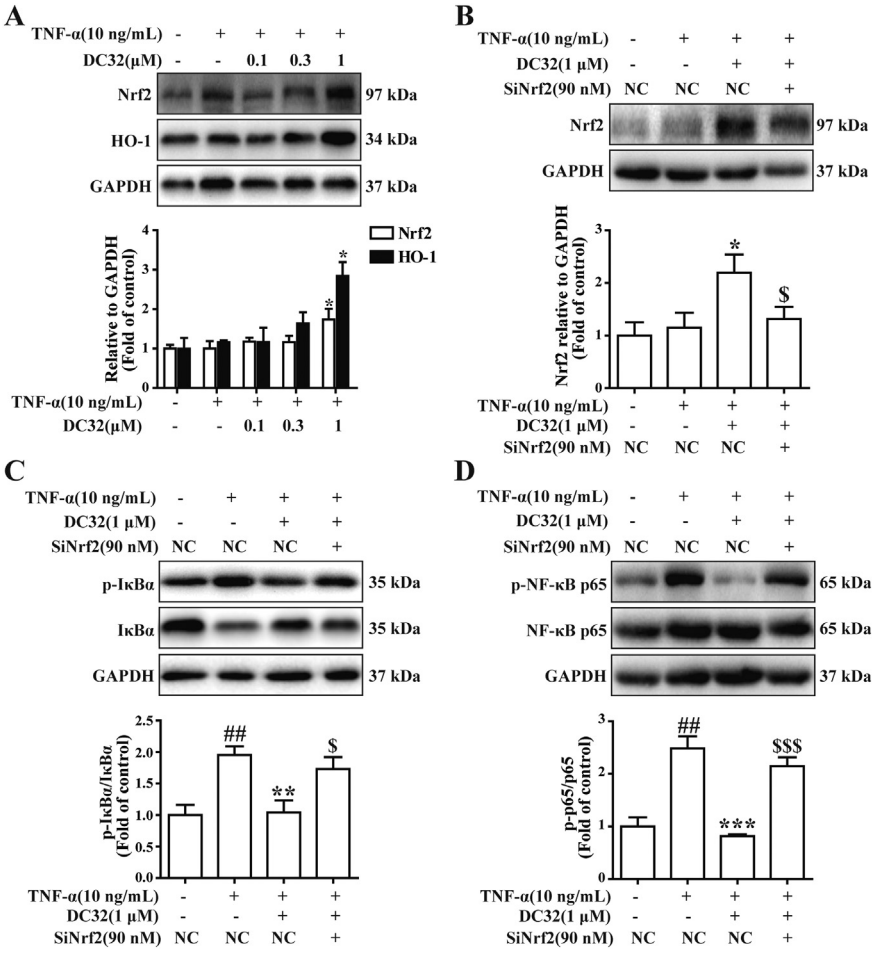

Fig. 4. DC32 inhibited NF-κB pathway by activating Nrf2 in cultured OA-FLSs. OA-FLSs of papain-induced OA rats were isolated and cultured. OA-FLSs were treated with TNF-α (10 ng/mL) and various concentrations of DC32 (0.1, 0.3 and 1 μM) for 24 h. The expression of Nrf2 and HO-1 were analyzed by western blot. DC32 (1 μM) significantly increased the protein levels of Nrf2 and HO-1 in OA-FLSs (A). OA-FLSs was transfected with Nrf2 siRNA for 24 h and then treated with DC32 (1 μM) for another 24 h. DC32 results in an increase of Nrf2 which could relieved by Nrf2 siRNA (B). DC32 inhibited the phosphorylation and degradation of IκBα, and the decrease of p-IκBα could relieved by Nrf2 siRNA (C). DC32 inhibited the phosphorylation of NF-κB p65, and the decrease of p-NF-κB p65 could relieved by Nrf2 siRNA (D). The data generated are from 3 replicate experiments. n = 5, values are the mean ± SEM. $^{\#\#}P < 0.01$, $^{\#\#\#}P < 0.001$ vs. the Control group, $^{*}P < 0.05$, $^{**}P < 0.01$, $^{***}P < 0.001$ vs. the TNF-α group, $^{\$}P < 0.05$, $^{\$\$\$}P < 0.001$ vs. the DC32 group.

2.11. Preparation of serum and ELISA assay

Blood samples were collected from the retro-orbital venous plexus. After standing for 30 min at room temperature, the samples were centrifuged at 2000 ×*g* for 15 min. The level of TNF-α (FMS-ELM028, FCMACS, China) in the serum was detected by ELISA kits.

2.12. mRNA isolation and quantitative real-time PCR (qPCR)

Isolation of total RNA from knee joints of C57BL/6J mice and OA-FLSs was performed using TransZol Up (ET111, Transgen, China). RNA quantity and quality were assessed in a NanoDrop-100 spectrophotometer (Thermo Scientific, USA). cDNA Reverse Transcription Kit (Hiscript II Reverse Transcriptase, R223-01, Vazyme, China) was used to reverse transcribe total RNA (1 μg) according to the manufacturers' instructions.

For quantification of gene expression by qPCR, SYBR Green detection chemistry (Q331-02, Vazyme, China) was used on the QuantStudio Real-Time PCR system (Thermo Scientific, USA). The cycling conditions included an initial step at 95 °C for 5 min, followed by 40 cycles at 95 °C for 10 s and 55–72 °C for 40 s. Quantitative measurements of all primers used in this study were determined using ($2^{-\Delta\Delta Ct}$) method. All values were expressed relative to the expression of GAPDH. Primer's sequences of the targeted genes were listed in Table 1.

2.13. Western blot analysis

Antibodies: anti-TNF-α antibody was purchased from Biorbyt (UK); antibodies against ERK, p-ERK, p38, p-p38, JNK, p-JNK, IκBα, p-IκBα, NF-κB p65, p-NF-κB p65, Nrf2, HRP-conjugated anti-rabbit IgG or anti-mouse IgG were purchased from CST (USA); anti-HO-1 antibody was purchased from Abcam (UK); and anti-GAPDH antibody was purchased from Sigma (USA).

The OA-FLSs were washed with PBS and knee joints from C57BL/6J mice were homogenized in liquid N2. Then, the OA-FLSs and homogenate were respectively suspended in 1 mL of ice-cold RIPA lysis buffer (Beyotime Biotechnology, China) with 10 μL of PMSF for 30 min for complete lysis. After centrifugation at 10,000 ×*g* for 15 min at 4 °C, the supernatants were transferred to new tubes. All extraction procedures were performed on ice. Protein concentrations were then determined using a BCA protein assay kit (Thermo Scientific, USA).

The samples were loaded onto a gel at 30 μg per lane for 10% sodium dodecyl sulfate-polyacrylamide gel electrophoresis and transferred onto a PVDF membrane (0.22 μm, Merk Millipore). After blocking with 5% nonfat dry milk for 2 h, the membrane was incubated with the primary antibody (1:1000) for overnight at 4 °C and then with the secondary antibody (1:4000) for 2 h. Later bands were visualized by exposure to ECL method and the overall gray value of protein bands (average gray value area) was quantified, GAPDH as internal marker. In brief, the target protein gray value/internal reference overall gray value was calculated.

2.14. Statistical analysis

All experiments were performed in triplicate. Statistical analysis was performed using GraphPad Prism 6.0 Software (San Diego, CA, USA). Data are presented as the mean ± SEM. Group comparisons were assessed with the two-tailed Student's *t*-test or ANOVA with Bonferroni's post hoc test for comparison of multiple columns. A value of $P < 0.05$ was considered as statistically significant.

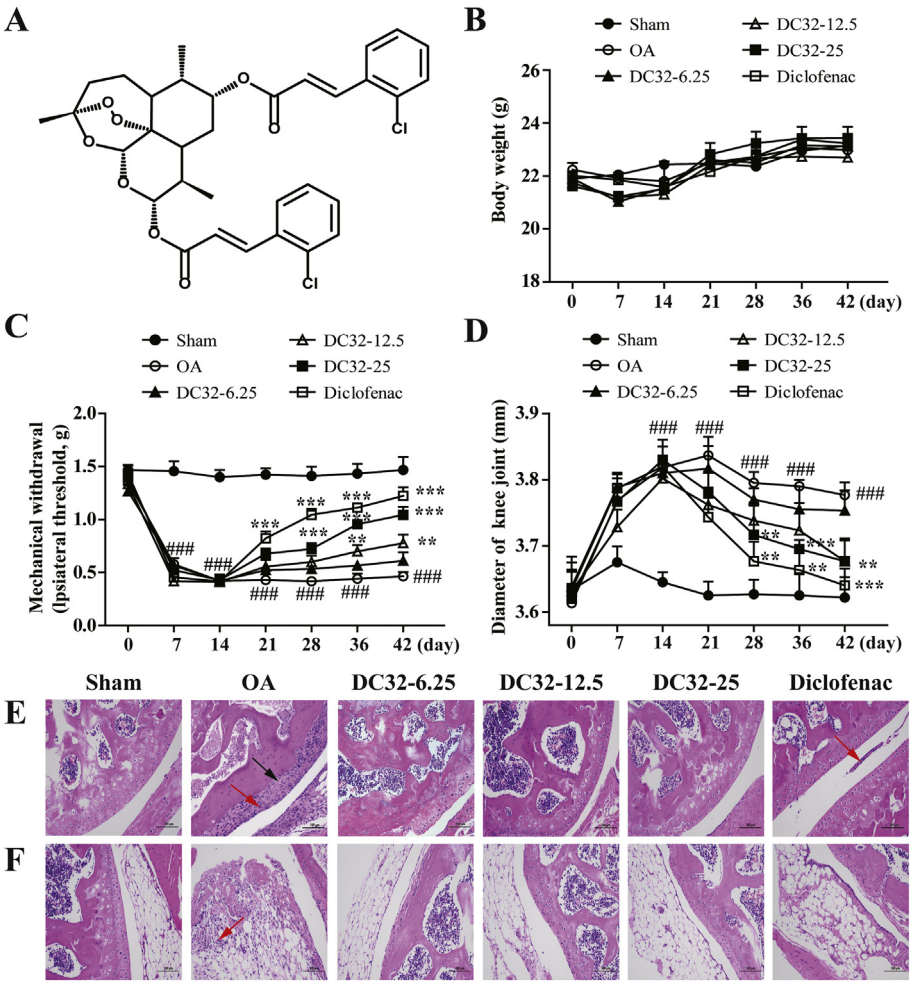

Fig. 5. DC32 ameliorated the symptoms of papain-induced OA mice. Chemical structure of DC32 (A). Papain-induced OA model was established in mice and different groups of mice were orally administered the vehicle, DC32 (6.25, 12.5, 25 mg/kg) or diclofenac sodium (1 mg/kg) from day 14 to day 42. The body weight of the mice was measured every week and had no difference in different groups (B). The mechanical withdrawal threshold of the mice of OA group in the feet decreased compared with that of the Sham group. Administration of DC32 and diclofenac sodium significantly alleviated papain-induced mechanical allodynia (C). The diameter of knee joint was measured every week and reduced by DC32 (D). Representative photographs of H&E-stained sections of cartilage (E) and synovium (F) in knee joints. The red arrow indicates inflammatory cell infiltration, and the black arrow indicates hyperplasia of connective tissues. The data generated are from 3 replicate experiments and the results are shown as an average ± SEM of 6 mice for each group. $^{###}P < 0.001$ vs. the Sham group, $^{*}P < 0.05$, $^{**}P < 0.01$, $^{***}P < 0.001$ vs. the OA group. (For interpretation of the references to colour in this figure legend, the reader is referred to the web version of this article.)

3. Results

3.1. DC32 reduced the transcription of pro-inflammatory cytokines and chemokines in cultured OA-FLSs

First, we analyzed the effect of DC32 on TNF-α-induced pro-inflammatory cytokines and chemokines production in cultured OA-FLSs. TNF-α significantly increased the mRNA levels of IL-6 (Fig. 1A) and IL-1β (Fig. 1B) in cultured OA-FLSs, and DC32 (0.1, 0.3, 1 μM) reversed this effect caused by TNF-α. In addition, DC32 (0.1, 0.3, 1 μM) significantly decreased the transcription of CXCL12 (Fig. 1C) and CX3CL1 (Fig. 1D) in cultured OA-FLSs, which were upregulated by TNF-α.

3.2. DC32 inhibited the migration and invasion of cultured OA-FLSs

A Transwell assay was used to determine whether DC32 could inhibit the migration and invasion of cultured OA-FLSs induced by TNF-α. Compared with the Control group, TNF-α significantly increased the migration and invasion of cultured OA-FLSs (Fig. 2A). The migration (Fig. 2B) and invasion ability (Fig. 2C) of OA-FLSs treated with different concentrations of DC32 was significantly decreased, which demonstrated a significant dose-dependent inhibition of cultured OA-FLSs migration and invasion.

3.3. DC32 inhibited the activation of ERK and NF-κB in cultured OA-FLSs

To further investigate the molecular mechanism through which DC32 inhibited TNF-α-induced inflammatory response in cultured OA-FLSs, western blot was performed to study changes in MAPK and NF-κB signaling pathways. As shown in Fig. 3A, DC32 (0.1–1 μM) had no cytotoxicity on cultured OA-FLSs and were used in this study. DC32 significantly inhibited the phosphorylation of ERK (Fig. 3B), but had no influence on the phosphorylation of p38 (Fig. 3C) or JNK (Fig. 3D). On the other hand, TNF-α stimulation dramatically increased the phosphorylation and degradation of IκBα and activated NF-kB p65 compared with the Control group. Oppositely, DC32 inhibited TNF-α-induced phosphorylation and degradation of IκBα (Fig. 3E), and decreased the phosphorylation of NF-κB p65 (Fig. 3F).

3.4. DC32 inhibited NF-κB pathway by activating Nrf2 in cultured OA-FLSs

The effect of DC32 on Nrf2/HO-1 pathway in cultured OA-FLSs was examined by western blot. DC32 (0.1, 0.3, 1 μM) was given to cultured OA-FLSs for 24 h, and the protein levels of HO-1 and Nrf2 were significantly upregulated in a dose-dependent manner (Fig. 4A). To verify the role of Nrf2 in the expression of NF-κB, siRNA for Nrf2 was transfected into cultured OA-FLSs (Fig. 4B). The change in the protein levels of IκBα and NF-κB p65 were determined by western blot. The results showed that Nrf2 siRNA could reverse the decrease in the phosphorylation of IκBα (Fig. 4C) and NF-κB p65 (Fig. 4D) induced by DC32.

3.5. DC32 ameliorated the symptoms of papain-induced OA mice

To evaluate whether DC32 has protective effect against induction and development of OA, papain-induced OA model was established in C57BL/6J mice. DC32 and diclofenac sodium were given to papain-induced OA mice from day 14 to day 42. The body weight and diameter of knee joint were measured every week to evaluate the therapeutic

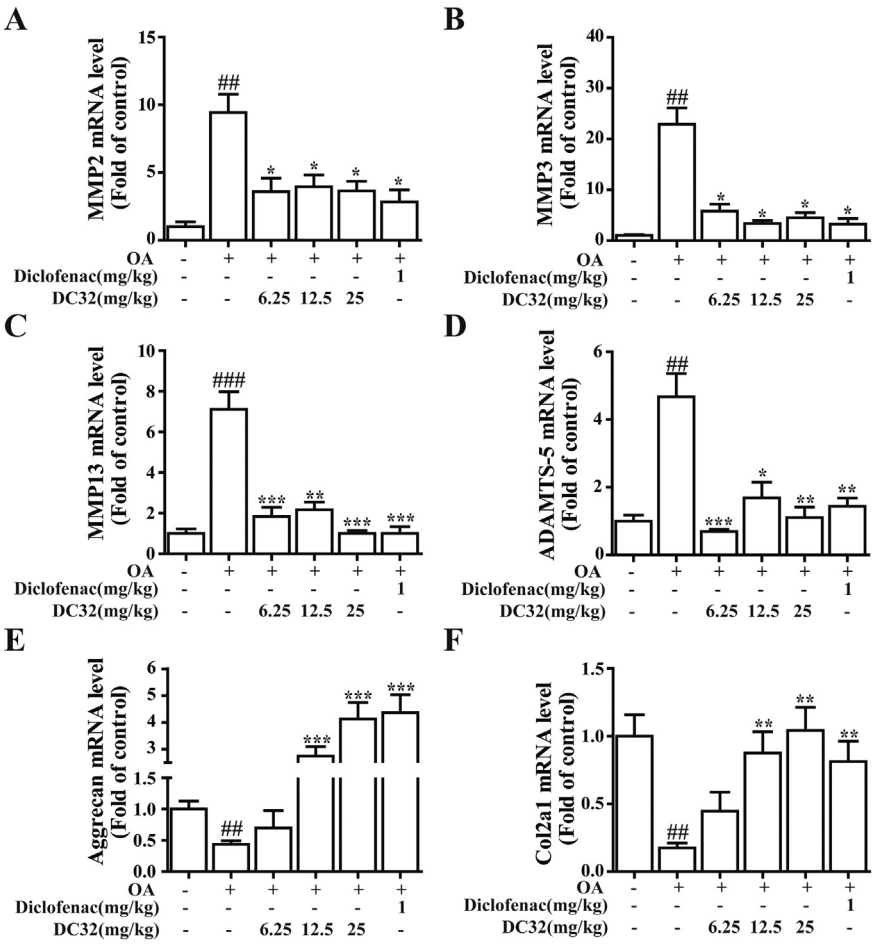

Fig. 6. DC32 reduced the transcription of MMPs and ADAMTS-5, increased that of aggrecan and Col2a1 in knee joint of papain-induced OA mice. Papain-induced OA model was established in mice and different groups of mice were orally administered the vehicle, DC32 (6.25, 12.5, 25 mg/kg) or diclofenac sodium (1 mg/kg) from day 14 to day 42. The relative levels of MMP2 (A), MMP3 (B), MMP13 (C), ADAMTS-5 (D), aggrecan (E) and Col2a1 (F) mRNA expression in the knee joint of papain-induced OA mice were measured by qPCR. The data generated are from 3 replicate experiments. n = 5, values are the mean ± SEM. $^{\#\#}P < 0.01$, $^{\#\#\#}P < 0.001$ vs. the Sham group, $^{*}P < 0.05$, $^{**}P < 0.01$, $^{***}P < 0.001$ vs. the OA group.

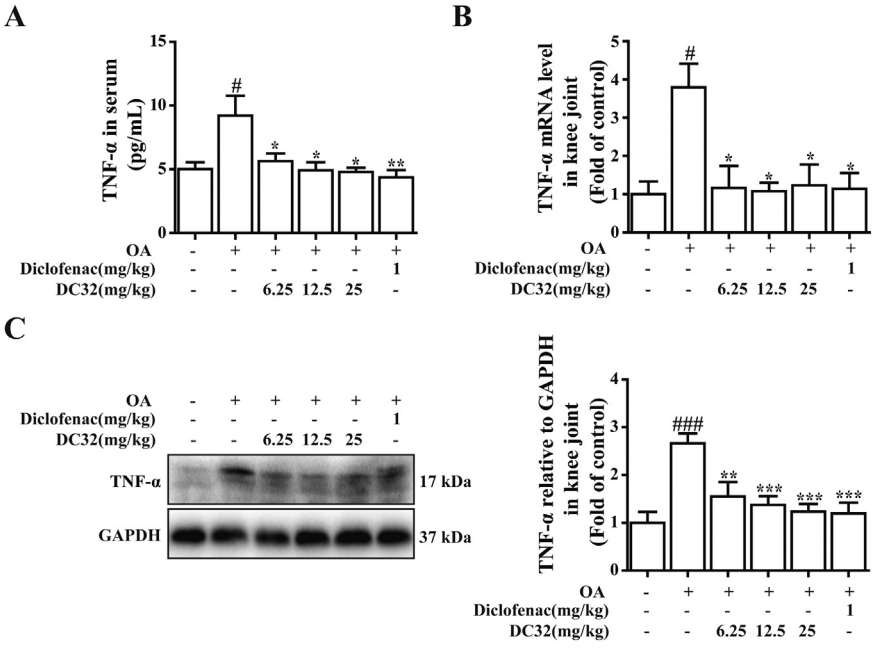

Fig. 7. DC32 reduced the level of TNF-α in the serum and knee joint of papain-induced OA mice. Papain-induced OA model was established in mice and different groups of mice were orally administered the vehicle, DC32 (6.25, 12.5, 25 mg/kg) or diclofenac sodium (1 mg/kg) from day 14 to day 42. The concentration of TNF-α in the serum was measured by ELISA and DC32 administration decreased the TNF-α level in the serum (A). The TNF-α mRNA level (B) and protein expression (C) were measured by qPCR and western blot. The data generated are from 3 replicate experiments. n = 5, values are the mean ± SEM. $^{\#}P < 0.05$, $^{\#\#\#}P < 0.001$ vs. the Sham group, $^{*}P < 0.05$, $^{**}P < 0.01$, $^{***}P < 0.001$ vs. the OA group.

effect of DC32 on OA. When the mice received an intra-articular injection of L-cysteine-activated papain, the body weight slightly decreased at first and then increased until no difference with the Sham group mice (Fig. 5B). Administration of DC32 (12.5, 25 mg/kg) attenuated mechanical allodynia in papain-induced pain in a dose dependent manner, without tolerance and resistance (Fig. 5C). In addition, DC32 alleviated the knee joint swelling of OA mice and the diameter of the knee joint was remained smaller than that of the OA group during DC32 administration (Fig. 5D). These results suggested that DC32 attenuated papain-induced mechanical allodynia and knee

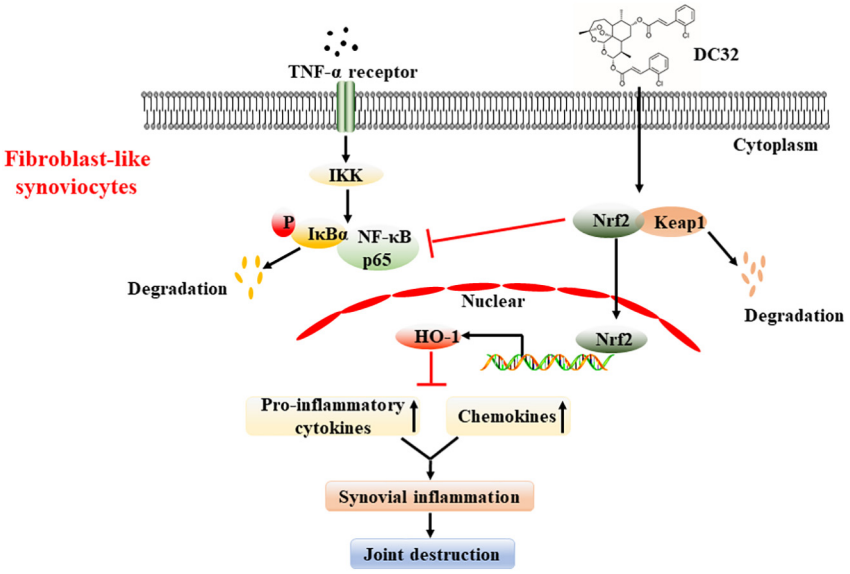

Fig. 8. Mechanisms of DC32-inhibited inflammatory response in osteoarthritic synovium. DC32 increased the expression of Nrf2 and then promoted HO-1 expression in cultured OA-FLSs. Furthermore, the activation of Nrf2 inhibited the degradation and phosphorylation of IκBα, which prevented the phosphorylation of NF-κB p65. In this way, DC32 inhibited the synovial inflammation in OA through reducing the production of pro-inflammatory cytokines and chemokines.

joint swelling in mice with OA. The H&E sections revealed that the knee joint in OA mice was seriously damaged by hyperplasia of connective tissues and inflammatory cell infiltration (Fig. 5E). However, there was almost no joint surface irregularity or erosion of the articular cartilage in DC32 treatment group except DC32-6.25 group. The synovium in OA mice was infiltrated with inflammatory cells and DC32 reduced the inflammatory cell infiltration (Fig. 5F). These data indicated that DC32 relieved inflammation and joint destruction caused by OA.

3.6. DC32 restored the balance of ECM biosynthetic and catabolic gene expression in knee joints of papain-induced OA mice

To examine the effect of DC32 on biosynthetic and catabolic gene expression in papain-induced OA mice, we detected the mRNA expression of MMP2, MMP3, MMP13, ADAMTS-5, aggrecan and Col2a1 by qPCR. MMP2 (Fig. 6A), MMP3 (Fig. 6B), MMP13 (Fig. 6C) and ADAMTS-5 (Fig. 6D) mRNA expression were significantly upregulated in the knee joints of OA mice, while the mRNA levels of aggrecan (Fig. 6E) and Col2a1 (Fig. 6F) were significantly downregulated. Administration of DC32 decreased the mRNA levels of MMPs and ADAMTS-5, and increased the mRNA levels of aggrecan and Col2a1.

3.7. DC32 reduced inflammation in papain-induced OA mice

Afterwards, we assessed the effect of DC32 on TNF-α expression in papain-induced OA mice. The level of TNF-α in serum were quantified by ELISA and the expression of TNF-α in knee joints were detected by qPCR and western blot. In mice with OA, the level of TNF-α in the serum (Fig. 7A) was almost twice high as that in the Sham group. Both the mRNA level (Fig. 7B) and the protein expression (Fig. 7C) of TNF-α in knee joints were significantly upregulated in papain-induced OA mice. All treatment groups significantly reduced the level of TNF-α in serum and the secretion of TNF-α in the knee joints.

4. Discussion

OA is characterized by cartilage breakdown and synovial inflammation, which is directly related to clinical symptoms such as joint swelling, synovitis and inflammatory pain [34]. As one of the drivers of OA pathogenesis, synovitis is initiated by the infiltration of inflammatory cells into the synovium, followed by synovial hyperplasia. The hyperplastic synovium produces pro-inflammatory cytokines, chemokines and proteases, and then invades and destroys cartilage. In particular, FLSs are central effectors of synovitis [35]. In this study, we investigated the effects of DC32 on inflammatory responses in rat osteoarthritic synovium and the protective effects of DC32 on papain-induced OA mice model.

Our results showed that DC32 inhibited the migration and invasion of OA-FLSs pretreated with TNF-α. Diclofenac sodium, a positive drug in this study, was commonly used for OA in clinic, while the overuse of diclofenac sodium could increase the risk of heart attacks in patients [36,37]. Compared with diclofenac sodium, DC32 dramatically reduced the transcription of IL-1β, IL-6, CXCL12 and CX3CL1 upregulated by TNF-α in cultured OA-FLSs. It was reported that inhibiting the production of chemokines may be a feasible therapeutic strategy to block the recruitment of inflammatory cells in synovitis [38]. These results suggested that DC32 inhibited inflammatory response in osteoarthritic synovium by reducing the production of pro-inflammatory cytokines and chemokines.

As a potent inducer of the inflammatory response, TNF-α activates the IKK/NF-κB and MAPK/AP-1 signaling pathways, which in turn trigger the production of pro-inflammatory cytokines and chemokines involved in the initiation and progression of inflammatory diseases, including OA [39,40]. The MAPK pathway can be divided into ERK, p38 and JNK MAPK pathways, which play an important role in phosphorylating transcription factors [41,42]. In our study, the phosphorylation of ERK, but not p38 and JNK, was suppressed by DC32. In general, ERK is mainly involved in anabolic processes, whereas JNK and p38 are mostly associated with cellular responses to stress conditions [43]. The ERK signaling pathway has been found to regulate diverse cellular processes such as proliferation, survival, differentiation and migration. It has been reported that the ERK signaling pathway, which induced the expression of MMP2, could be inhibited by several NSAIDs [44]. DC32 may therefore suppressed the anabolic processes regulated by ERK signaling pathway to inhibit inflammatory response in osteoarthritic synovium.

MAPK activates the NF-κB pathway to induce the expression of pro-inflammatory factors and infiltration of inflammatory cells [45,46]. Hence, we further investigated the effects of DC32 on NF-κB pathway. Under physiological conditions, NF-κB p65 is sequestered in the cytoplasm by the IκBα protein. Upon inflammatory stimulation, such as TNF-α, IKK promotes IκBα phosphorylation and degradation, which enables NF-κB p65 to translocate to the nucleus [47]. NF-κB p65 then binds to its specific promoter region and initiates the transcription of inflammatory factors [48]. Our results revealed that DC32 downregulated the phosphorylation of NF-κB p65 by decreasing the

phosphorylation and degradation of IκBα in OA-FLSs.

We have previously reported that DC32 ameliorated inflammatory symptoms by activating the Nrf2/HO-1 pathway in mice with CIA [25,26]. Nrf2, a key transcription factor, was reported to play a central role in protecting cells against oxidative stress and upregulating the genes encoding antioxidant proteins including HO-1 [49]. DC32 activated Nrf2 and then upregulated the expression of HO-1 in OA-FLSs. Deletion of Nrf2 enhanced inflammation, while its upregulation decreased pro-inflammatory and immune responses regulated by NF-κB [50]. Nrf2 prevented the degradation of IκBα and blocked NF-κB p65 nuclear translocation and transcription of pro-inflammatory genes sequentially. In this study, Nrf2 mRNA interference relieved the DC32-induced downregulation of IκBα and NF-κB p65, proving that the activation of Nrf2 inhibited the NF-κB pathway.

To further evaluate whether DC32 has protective effects on OA, we established papain-induced OA mice model for the in vivo study. The papain-induced OA mice developed joint inflammation, while DC32 showed good protective effects on knee joint swelling and inflammatory cell infiltration. And DC32 also attenuated the splenomegaly caused by OA (Fig. S1). We found that the body weight of the mice had no significant changes after intra-articular injection with papain compared with that of the Sham group. It is consistent with previous reports that the progression of OA may not continuously lead to weight loss, which might only occur in the early stages of OA [28].

Von Frey filaments were used to evaluate mechanical allodynia in papain-induced OA mice, and DC32 was found to attenuate papain-induced mechanical allodynia without tolerance or resistance. However, the mechanism underlying OA-related pain has not been fully illuminated [51]. Since the articular cartilage has no vessels or nerves, noncartilaginous joint tissues such as subchondral bone, periosteum, synovium, ligament and joint capsules are thought to be important in pain generation [51,52]. DC32 downregulated the mRNA levels of IL-1β and IL-6 in cultured OA-FLSs reported to contribute to the development of pain, potentially explaining the decreased pain perception in papain-induced OA mice [14].

DC32 significantly inhibited the cartilage degradation and inflammatory cell infiltration in synovium caused by OA, which was observed in H&E-stained sections. An imbalance of ECM biosynthesis and catabolism in articular cartilage was also observed in papain-induced OA mice. The reduced synthesis of ECM and the increased production of enzymes resulted in the acceleration of joint damage [53]. DC32 had an effect on the overall metabolism of proteoglycans in OA cartilage by promoting synthesis and reducing catabolic gene expression. Inflammatory cytokines promote the synthesis and release of proteolytic enzymes, which decompose the key components of ECM. Both IL-1β, IL-6 and TNF-α are considered to be dominant in the induction of inflammation and bone erosion [54]. DC32 decreased the level of TNF-α in serum and reduced the secretion of TNF-α in the knee joints of papain-induced OA mice. DC32 could not only inhibit inflammation by reducing the secretion of TNF-α, but also regulate cartilage biosynthesis and catabolic activity in treatment of OA.

In conclusion, our results demonstrated that DC32 suppressed the inflammatory response in osteoarthritic synovium through regulating Nrf2/NF-κB pathway (Fig. 8). Moreover, DC32 alleviated pain and inflammation, restored the balance of ECM biosynthetic and catabolic activities in papain-induced OA mice. DC32 exhibited same efficacy with diclofenac sodium in attenuating papain-induced OA and showed a higher therapeutic effect on osteoarthritic synovium. These findings suggest that DC32 may be a promising agent for the treatment of OA.

Supplementary data to this article can be found online at https://doi.org/10.1016/j.intimp.2019.105701.

Ethics approval

All animal welfare in this study was carried out in accordance with the recommendations of National Institutes of Health Guide for the Care and Use of Laboratory Animals, and the protocols used were approved by the Animal Ethics Committee of China Pharmaceutical University.

Availability of data and materials

The datasets supporting the conclusions of this article are included within the article.

Funding

This research was supported by Major National Science and Technology Program of China for Innovative Drug (2017ZX09101002-002-003).

Authors' contributions

YL designed and carried out the experiments, analyzed the data, and wrote and discussed the manuscript. MF assisted with the experiments and revised the manuscript. HL synthesized and purified the DC32 used in this study. BM assisted with the experiments. WD revised the manuscript. BY and JL reviewed the manuscript and supervised the project.

Declaration of Competing Interest

The authors declare that they have no competing interests.

References

[1] Y. Yang, Y. Wang, Y. Kong, X. Zhang, H. Zhang, Y. Gang, L. Bai, Carnosine prevents type 2 diabetes-induced osteoarthritis through the ROS/NF-kappaB pathway, Front. Pharmacol. 9 (2018) 598.
[2] S.C. Gemma Wallace, C. Do, L. King, S. Kluzek, A. Price, F. Roemer, A. Guermazi, R. Keen, N. Arden, Associations between clinical evidence of inflammation and synovitis in symptomatic knee osteoarthritis: a cross-sectional substudy, Arthritis Care Res. 69 (9) (2017) 1340–1348.
[3] D.T. Felson, J. Niu, T. Neogi, J. Goggins, M.C. Nevitt, F. Roemer, J. Torner, C.E. Lewis, A. Guermazi, M.I. Group, Synovitis and the risk of knee osteoarthritis: the MOST Study, Osteoarthr. Cartil. 24 (3) (2016) 458–464.
[4] L.A. MacFarlane, H. Yang, J.E. Collins, M. Jarraya, A. Guermazi, L.A. Mandl, S.D. Martin, J. Wright, E. Losina, J.N. Katz, O.R.I.G. MeTe, Association of changes in effusion-synovitis with progression of cartilage damage over eighteen months in patients with osteoarthritis and meniscal tear, Arthritis Rheumatol. 71 (1) (2019) 73–81.
[5] M.B. Goldring, S.R. Goldring, Osteoarthritis, J. Cell. Physiol. 213 (3) (2007) 626–634.
[6] R.F. Loeser, Molecular mechanisms of cartilage destruction: mechanics, inflammatory mediators, and aging collide, Arthritis Rheum. 54 (5) (2006) 1357–1360.
[7] A. Mathiessen, P.G. Conaghan, Synovitis in osteoarthritis: current understanding with therapeutic implications, Arthritis Res. Ther. 19 (1) (2017) 18.
[8] I. Prieto-Potin, R. Largo, J.A. Roman-Blas, G. Herrero-Beaumont, D.A. Walsh, Characterization of multinucleated giant cells in synovium and subchondral bone in knee osteoarthritis and rheumatoid arthritis, BMC Musculoskelet. Disord. 16 (2015) 226.
[9] K.-W. IR, Inflammatory cells in patients with endstage knee osteoarthritis: a comparison between the synovium and the infrapatellar fat pad, J. Rheumatol. 43 (4) (2016) 771–778.
[10] B.J. de Lange-Brokaar, A. Ioan-Facsinay, G.J. van Osch, A.M. Zuurmond, J. Schoones, R.E. Toes, T.W. Huizinga, M. Kloppenburg, Synovial inflammation, immune cells and their cytokines in osteoarthritis: a review, Osteoarthr. Cartil. 20 (12) (2012) 1484–1499.
[11] M. Balan, S. Pal, A novel CXCR3-B chemokine receptor-induced growth-inhibitory signal in cancer cells is mediated through the regulation of Bach-1 protein and Nrf2 protein nuclear translocation, J. Biol. Chem. 289 (6) (2014) 3126–3137.
[12] Y. Zou, S. Zeng, M. Huang, Q. Qiu, Y. Xiao, M. Shi, Z. Zhan, L. Liang, X. Yang, H. Xu, Inhibition of 6-phosphofructo-2-kinase suppresses fibroblast-like synoviocytes-mediated synovial inflammation and joint destruction in rheumatoid arthritis, Br. J. Pharmacol. 174 (9) (2017) 893–908.
[13] L.E. Hand, S.H. Dickson, A.J. Freemont, D.W. Ray, J.E. Gibbs, The circadian regulator Bmal1 in joint mesenchymal cells regulates both joint development and inflammatory arthritis, Arthritis Res. Ther. 21 (1) (2019) 5.
[14] P. Wojdasiewicz, L.A. Poniatowski, D. Szukiewicz, The role of inflammatory and anti-inflammatory cytokines in the pathogenesis of osteoarthritis, Mediat. Inflamm. 2014 (2014) 561459.
[15] K.B. Marcu, M. Otero, E. Olivotto, R.M. Borzi, M.B. Goldring, NF-kappaB signaling: multiple angles to target OA, Curr. Drug Targets 11 (5) (2010) 599–613.

[16] C. Cheng, W. Shan, W. Huang, Z. Ding, G. Cui, F. Liu, W. Lu, J. Xu, W. He, Z. Yin, ACY-1215 exhibits anti-inflammatory and chondroprotective effects in human osteoarthritis chondrocytes via inhibition of STAT3 and NF-kappaB signaling pathways, Biomed. Pharmacother. 109 (2019) 2464–2471.
[17] A. Alquraini, M. Jamal, L. Zhang, T. Schmidt, G.D. Jay, K.A. Elsaid, The autocrine role of proteoglycan-4 (PRG4) in modulating osteoarthritic synoviocyte proliferation and expression of matrix degrading enzymes, Arthritis Res. Ther. 19 (1) (2017) 89.
[18] M.B. Goldring, Chondrogenesis, chondrocyte differentiation, and articular cartilage metabolism in health and osteoarthritis, Ther. Adv. Musculoskelet. Dis. 4 (4) (2012) 269–285.
[19] X. Song, M. Zhu, H. Li, B. Liu, Z. Yan, W. Wang, H. Li, J. Sun, S. Li, USF1 promotes the development of knee osteoarthritis by activating the NF-kappaB signaling pathway, Exp. Ther. Med. 16 (4) (2018) 3518–3524.
[20] Y.Q. Qian, Z.H. Feng, X.B. Li, Z.C. Hu, J.W. Xuan, X.Y. Wang, H.C. Xu, J.X. Chen, Downregulating PI3K/Akt/NF-kappaB signaling with allicin for ameliorating the progression of osteoarthritis: in vitro and vivo studies, Food Funct. 9 (9) (2018) 4865–4875.
[21] S.M. Hou, C.H. Hou, J.F. Liu, CX3CL1 promotes MMP-3 production via the CX3CR1, c-Raf, MEK, ERK, and NF-kappaB signaling pathway in osteoarthritis synovial fibroblasts, Arthritis Res. Ther. 19 (1) (2017) 282.
[22] W. Li, T.O. Khor, C. Xu, G. Shen, W.S. Jeong, S. Yu, A.N. Kong, Activation of Nrf2-antioxidant signaling attenuates NFkappaB-inflammatory response and elicits apoptosis, Biochem. Pharmacol. 76 (11) (2008) 1485–1489.
[23] D. Zhao, J. Zhang, G. Xu, Q. Wang, Artesunate protects LPS-induced acute lung injury by inhibiting TLR4 expression and inducing Nrf2 activation, Inflammation 40 (3) (2017) 798–805.
[24] T. Li, H. Chen, Z. Yang, X.G. Liu, L.M. Zhang, H. Wang, Evaluation of the immunosuppressive activity of artesunate in vitro and in vivo, Int. Immunopharmacol. 16 (2) (2013) 306–312.
[25] M. Fan, Y. Li, C. Yao, X. Liu, J. Liu, B. Yu, DC32, a dihydroartemisinin derivative, ameliorates collagen-induced arthritis through an Nrf2-p62-Keap1 feedback loop, Front. Immunol. 9 (2018) 2762.
[26] M. Fan, Y. Li, C. Yao, X. Liu, X. Liu, J. Liu, Dihydroartemisinin derivative DC32 attenuates collagen-induced arthritis in mice by restoring the Treg/Th17 balance and inhibiting synovitis through down-regulation of IL-6, Int. Immunopharmacol. 65 (2018) 233–243.
[27] C.C. Xu, T. Deng, M.L. Fan, W.B. Lv, J.H. Liu, B.Y. Yu, Synthesis and in vitro antitumor evaluation of dihydroartemisinin-cinnamic acid ester derivatives, Eur. J. Med. Chem. 107 (2016) 192–203.
[28] S. Panicker, J. Borgia, C. Fhied, K. Mikecz, T.R. Oegema, Oral glucosamine modulates the response of the liver and lymphocytes of the mesenteric lymph nodes in a papain-induced model of joint damage and repair, Osteoarthr. Cartil. 17 (8) (2009) 1014–1021.
[29] Y.J. Wang, M. Shen, S. Wang, X. Wen, X.R. Han, Z.F. Zhang, H. Li, F. Wang, D.M. Wu, J. Lu, Y.L. Zheng, Inhibition of the TGF-beta1/Smad signaling pathway protects against cartilage injury and osteoarthritis in a rat model, Life Sci. 189 (2017) 106–113.
[30] S. Yin, P. Wang, R. Xing, L. Zhao, X. Li, L. Zhang, Y. Xiao, Transient receptor potential ankyrin 1 (TRPA1) mediates lipopolysaccharide (LPS)-induced inflammatory responses in primary human osteoarthritic fibroblast-like synoviocytes, Inflammation 41 (2) (2018) 700–709.
[31] W. Zhu, C. Jiang, J. Xu, M. Geng, X. Wu, J. Sun, J. Ma, R. Holmdahl, L. Meng, S. Lu, Pristane primed rat T cells enhance TLR3 expression of fibroblast-like synoviocytes via TNF-alpha initiated p38 MAPK and NF-kappaB pathways, Clin. Immunol. 156 (2) (2015) 141–153.
[32] M. Lin, Y. Lin, X. Li, W. Liang, S. Wang, J. Liu, X. Liu, L. Chen, Y. Qin, Warm sparse-dense wave inhibits cartilage degradation in papain-induced osteoarthritis through the mitogen-activated protein kinase signaling pathway, Exp. Ther. Med. 14 (4) (2017) 3674–3680.
[33] C.B. Knights, C. Gentry, S. Bevan, Partial medial meniscectomy produces osteoarthritis pain-related behaviour in female C57BL/6 mice, Pain 153 (2) (2012) 281–292.
[34] C.R. Scanzello, S.R. Goldring, The role of synovitis in osteoarthritis pathogenesis, Bone 51 (2) (2012) 249–257.
[35] J.H. Lee, B. Kim, W.J. Jin, H.H. Kim, H. Ha, Z.H. Lee, Pathogenic roles of CXCL10 signaling through CXCR3 and TLR4 in macrophages and T cells: relevance for arthritis, Arthritis Res. Ther. 19 (1) (2017) 163.
[36] M. Rahmati, A. Mobasheri, M. Mozafari, Inflammatory mediators in osteoarthritis: a critical review of the state-of-the-art, current prospects, and future challenges, Bone 85 (2016) 81–90.
[37] Y.S. Ou, C. Tan, H. An, D.M. Jiang, Z.X. Quan, K. Tang, X.J. Luo, The effects of NSAIDs on types I, II, and III collagen metabolism in a rat osteoarthritis model, Rheumatol. Int. 32 (8) (2012) 2401–2405.
[38] T. Nanki, T. Imai, S. Kawai, Fractalkine/CX3CL1 in rheumatoid arthritis, Mod. Rheumatol. 27 (3) (2017) 392–397.
[39] T. Xu, T. Ying, L. Wang, X.D. Zhang, Y. Wang, L. Kang, T. Huang, L. Cheng, L. Wang, Q. Zhao, A native-like bispecific antibody suppresses the inflammatory cytokine response by simultaneously neutralizing tumor necrosis factor-alpha and interleukin-17A, Oncotarget 8 (47) (2017) 81860–81872.
[40] Y. Wang, J. Cao, Y. Fan, Y. Xie, Z. Xu, Z. Yin, L. Gao, C. Wang, Artemisinin inhibits monocyte adhesion to HUVECs through the NF-kappaB and MAPK pathways in vitro, Int. J. Mol. Med. 37 (6) (2016) 1567–1575.
[41] Z.C. Lin, C.W. Lee, M.H. Tsai, H.H. Ko, J.Y. Fang, Y.C. Chiang, C.J. Liang, L.F. Hsu, S.C. Hu, F.L. Yen, Eupafolin nanoparticles protect HaCaT keratinocytes from particulate matter-induced inflammation and oxidative stress, Int. J. Nanomedicine 11 (2016) 3907–26.
[42] P. Chandrakesan, I. Ahmed, T. Anwar, Y. Wang, S. Sarkar, P. Singh, S. Peleg, S. Umar, Novel changes in NF-{kappa}B activity during progression and regression phases of hyperplasia: role of MEK, ERK, and p38, J. Biol. Chem. 285 (43) (2010) 33485–33498.
[43] J. Sun, R.D. Ramnath, L. Zhi, R. Tamizhselvi, M. Bhatia, Substance P enhances NF-kappaB transactivation and chemokine response in murine macrophages via ERK1/2 and p38 MAPK signaling pathways, Am. J. Physiol. Cell Physiol. 294 (6) (2008) C1586–C1596.
[44] M.R. Pan, H.C. Chang, W.C. Hung, Non-steroidal anti-inflammatory drugs suppress the ERK signaling pathway via block of Ras/c-Raf interaction and activation of MAP kinase phosphatases, Cell. Signal. 20 (6) (2008) 1134–1141.
[45] J. Wang, J. Huang, L. Wang, C. Chen, D. Yang, M. Jin, C. Bai, Y. Song, Urban particulate matter triggers lung inflammation via the ROS-MAPK-NF-kappaB signaling pathway, J. Thorac. Dis. 9 (11) (2017) 4398–4412.
[46] W. Liu, S. Huang, Y. Li, Y. Li, D. Li, P. Wu, Q. Wang, X. Zheng, K. Zhang, Glycyrrhizic acid from licorice down-regulates inflammatory responses via blocking MAPK and PI3K/Akt-dependent NF-kappaB signalling pathways in TPA-induced skin inflammation, Medchemcomm 9 (9) (2018) 1502–1510.
[47] W.D. Li, Y.J. Dong, Y.Y. Tu, Z.B. Lin, Dihydroarteannuin ameliorates lupus symptom of BXSB mice by inhibiting production of TNF-alpha and blocking the signaling pathway NF-kappa B translocation, Int. Immunopharmacol. 6 (8) (2006) 1243–1250.
[48] C. Zoja, A. Benigni, G. Remuzzi, The Nrf2 pathway in the progression of renal disease, Nephrol. Dial. Transplant. 29 (Suppl. 1) (2014) i19–i24.
[49] M. Buelna-Chontal, C. Zazueta, Redox activation of Nrf2 & NF-kappaB: a double end sword? Cell. Signal. 25 (12) (2013) 2548–2557.
[50] F. Sivandzade, S. Prasad, A. Bhalerao, L. Cucullo, NRF2 and NF-B interplay in cerebrovascular and neurodegenerative disorders: molecular mechanisms and possible therapeutic approaches, Redox Biol. 21 (2018) 101059.
[51] J. Lee, Y.S. Hong, J.H. Jeong, E.J. Yang, J.Y. Jhun, M.K. Park, Y.O. Jung, J.K. Min, H.Y. Kim, S.H. Park, M.L. Cho, Coenzyme Q10 ameliorates pain and cartilage degradation in a rat model of osteoarthritis by regulating nitric oxide and inflammatory cytokines, PLoS One 8 (7) (2013) e69362.
[52] D.B. Mach, S.D. Rogers, M.C. Sabino, N.M. Luger, M.J. Schwei, J.D. Pomonis, C.P. Keyser, D.R. Clohisy, D.J. Adams, P. O'Leary, P.W. Mantyh, Origins of skeletal pain: sensory and sympathetic innervation of the mouse femur, Neuroscience 113 (1) (2002) 155–166.
[53] P. Wang, P.P. Guan, C. Guo, F. Zhu, K. Konstantopoulos, Z.Y. Wang, Fluid shear stress-induced osteoarthritis: roles of cyclooxygenase-2 and its metabolic products in inducing the expression of proinflammatory cytokines and matrix metalloproteinases, FASEB J. 27 (12) (2013) 4664–4677.
[54] Y. Chang, X. Jia, X. Sun, S. Xu, Y. Wu, L. Zhang, W. Wei, APRIL promotes proliferation, secretion and invasion of fibroblast-like synoviocyte from rats with adjuvant induced arthritis, Mol. Immunol. 64 (1) (2015) 90–98.